ISSN: 2588-4115; Infection Epidemiology and Microbiology. 2026;12(3):191-214 doi 10.52547/iem.12.3.191

Proteomics Exploration of *Helicobacter pylori* to Design an Innovative Multi-Epitope mRNA Vaccine

ARTICLE INFO

Article Type
Original Article

Authors
Mohammad Hossein Maleki, *PhD*[1]
Nourkhoda Sadeghifard, *PhD*[2]
Saeed Khoshnood, *PhD*[2]
Nazanin Omidi, *MSc*[2]
Mohammad Yazdanmanesh, *MSc*[2]
Behrooz Sadeghi Kalani, *PhD*[1,3]*

[1] Student Research Committee, Ilam University of Medical Sciences, Ilam, Iran
[2] Clinical Microbiology Research Center, Ilam University of Medical Sciences, Ilam, Iran
[3] Department of Microbiology, Faculty of Medicine, Iran University of Medical Sciences, Ilam, Iran

**** Correspondence***
Department of Microbiology, Faculty of Medicine, Iran University of Medical Sciences, Ilam, Iran.
E-mail: Sadeghi-b@medilam.ac.ir

How to cite this article
Maleki M.H., Sadeghifard N., Khoshnood S., Omidi N., Yazdanmanesh M., Sadeghi Kalani B. Proteomics Exploration of Helicobacter pylori to Design an Innovative Multi-Epitope mRNA Vaccine. Infection Epidemiology and Microbiology. 2026;12(3): 191-214.

Article History
Received: August 30, 2025
Revised: June 30, 2026
Accepted: July 14, 2026
Published: July 27, 2026

ABSTRACT

Background: This study aimed to explore the virulence factors associated with *Helicobacter pylori* and develop a multi-epitope vaccine.
Materials & Methods: Several antigenic proteins derived from the *H. pylori* proteome were analyzed, including *CagA*, *FlaA*, *FlaB*, *OipA*, *SabA*, *UreA*, *HSP*, *BabA*, and *FecA*. B and T cell epitopes were predicted for HTL, CTL, and B cells. Predicted stability and immunological responses to the vaccine were assessed using molecular binding analysis, thermodynamic sketching, in silico expression assessments, and agent-based modeling.
Findings: This study identified and selected B-cell epitopes from eight *H. pylori* proteins using the ABCpred web server, resulting in 19 epitopes after filtering for allergenic, toxic, and homologous properties. Computationally, the epitopes from *BabA*, *CagA*, and *FlaA* showed favorable scores and no adverse characteristics. Additionally, 20 CTL epitopes and 17 HTL epitopes were selected based on their IC_{50} values and conservation within protein sequences. Molecular docking predicted that the epitope LSDGAAAGY had the highest binding affinity to the MHC allele HLA-A*01:01, achieving -643.6 kcal/moL, suggesting potential for vaccine development.
Conclusion: This computational study supports the strategic assembly of epitopes for multi-epitope vaccine design, providing in silico insights requiring experimental validation for future *H. pylori* interventions

Keywords: *H. pylori,* Vaccine, Epitopes, Molecular docking, Helper T lymphocyte

CITATION LINKS

[1] Yi, M., et al., Helicobacter pylori... [2] Duan, Y., et al., Helicobacter pylori... [3] Ali, A. and K.I. AlHussaini, Helicobacter pylori:... [4] Elbehiry, A., et al., Helicobacter pylori... [5] Ibrahim, M.E., Epidemiology, pathogenicity... [6] Mladenova, I., Review–Epidemiology of... [7] Wizenty, J. and M. Sigal, Helicobacter pylori... [8] Sun, Q., et al., Helicobacter pylori infection... [9] Chey, W.D., et al., ACG clinical guideline... [10] Kadhim, A.S. and A.S. Al-Karawi, Insights into... [11] Sharndama, H.C. and I.E. Mba, Helicobacter pylori... [12] Wang, H., et al., A review of signal... [13] Liu, S., et al., Helicobacter pylori CagA... [14] Karbalaei, M., A. Talebi Bezmin Abadi, and M. Keikha, Clinical... [15] Son, Y.S., et al., Helicobacter pylori VacA... [16] Yunle, K., et al., Advances in... [17] Keshri, A.K., et al., Designing and... [18] Gong, J., et al., Helicobacter pylori vaccine... [19] Raman, S.K.S., et al., In silico... [20] Asadinezhad, M., et al., Development of... [21] Asadollahi, P. and B.S. Kalani, Novel... [22] Asadinezhad, M., et al., Proteomics exploration... [23] Fattahi, R., et al., Computational... [24] Fattahi, N., et al., Engineering... [25] Al-Sallami, D., et al., Design of... [26] Fattahi, R. and B. Sadeghi Kalani, mRNA vaccine... [27] Cruz, J., et al., BacMap: an up-to... [28] Sabzi, S., et al., Genome-wide... [29] Praveen, M., Multi-epitop... [30] Cui, M., et al., Design of a Helicobacter... [31] Alhassan, H.H., Advanced vaccinomic... [32] López-Blanco, J.R., et al., iMODS: internal... [33] Ghosh, P., et al., A novel multi... [34] Khan, M., et al., Immunoinformatics... [35] Barbier, A.J., et al., The clinical... [36] Pardi, N., et al., mRNA vaccines... [37] Shahrear, S. and A.B.M.M.K. Islam, Modeling...

Copyright@ 2026, TMU Press. This open-access article is published under the terms of the Creative Commons Attribution-NonCommercial 4.0 International License which permits Share (copy and redistribute the material in any medium or format) and Adapt (remix, transform, and build upon the material) under the Attribution-NonCommercial terms.

Introduction

Helicobacter pylori is a microaerophilic, Gram-negative bacterium characterized by its spiral morphology. This organism predominantly colonizes the gastric mucosa, where it plays a significant role in various gastrointestinal disorders, including chronic gastritis, peptic ulcers, and gastric cancer [1, 2]. *H. pylori* infection is associated with a wide range of gastrointestinal disorders. Notably, it is a primary etiological factor in the development of chronic gastritis, characterized by inflammation of the gastric mucosa. Additionally, *H. pylori* plays a significant role in the pathogenesis of peptic ulcers, which could lead to complications such as bleeding and perforation [2, 3]. *H. pylori* is predominantly acquired during childhood, with oral-oral contact being the most common transmission mode. This transmission route suggests that the bacterium could spread through saliva or other oral secretions, facilitating its establishment in the gastric mucosa of susceptible individuals [2-4]. Its prevalence ranges from 10 to 70% and could possibly reach 100% in poor nations [2, 5]. Recent investigations have indicated that *H. pylori* is responsible for approximately 75% of all gastric malignancies worldwide. This bacterium is classified as a Group I human carcinogen due to its established role in the development of gastric adenocarcinoma and mucosa-associated lymphoid tissue (MALT) lymphoma. Epidemiological studies have demonstrated a significant correlation between chronic *H. pylori* infection and an increased risk of these cancers, particularly in regions with high incidence rates of gastric malignancies [2, 6].

H. pylori has been designated as a Group 1 carcinogen in humans by the International Agency for Research on Cancer (IARC), a specialized agency of the World Health Organization (WHO). This classification, established in 1994, indicates that there is enough epidemiological evidence to support a definitive association between *H. pylori* infection and the development of gastric malignancies, particularly gastric adenocarcinoma and mucosa-associated lymphoid tissue (MALT) lymphoma [7, 8]. Current therapeutic regimens for *H. pylori* infections typically involve a triple therapy consisting of two antibiotics—either amoxicillin combined with clarithromycin or metronidazole—alongside a proton pump inhibitor (PPI). This combination aims to effectively eradicate the bacteria while managing gastric acidity, which enhances the efficacy of the antibiotics [8, 9]. Most cases of *H. pylori* infection could be effectively treated; however, several studies have reported concerning declines in the efficacy of standard antibiotic therapies. Specifically, eradication rates associated with typical triple therapy—comprising two antibiotics and a proton pump inhibitor—have decreased from approximately 90% to 70-80% in certain regions [8-10]. The decline in eradication rates associated with standard triple therapy for *H. pylori* infections is closely linked to the development of antibiotic-resistant strains in various nations. This decrease in eradication rates from approximately 90% to 70-80% poses significant challenges for effective treatment. As antibiotic resistance continues to complicate therapeutic options, progress in developing an effective vaccine against *H. pylori* is increasingly considered as a critical strategy for preventing and managing this infection [8].

Virulence-related surface proteins of *H. pylori*, an extracellular pathogen, play a crucial role in host-pathogen interactions and significantly contribute to its pathogenicity. These proteins facilitate flagella-driven motility, enabling *H. pylori* to navigate effectively through the gastric epithelial

layer. Virulence factors produced by *H. pylori* contribute to the development of chronic and progressive inflammation of the gastric mucosa. This persistent inflammatory response could lead to a series of pathological changes, including tissue necrosis, mucosal atrophy, and lesion formation. Over time, these alterations may progress to intestinal metaplasia, a precancerous condition that increases the likelihood of developing gastric cancer. Understanding the processes through which *H. pylori* virulence factors promote inflammation and tissue damage is essential for developing targeted therapeutic strategies aimed at preventing long-term complications associated with this infection, including gastric cancer. Continued research into the specific roles of these virulent proteins will enhance our knowledge of *H. pylori* pathogenesis and inform future interventions to mitigate its health impacts [11, 12]. *H. pylori* infection is increasingly prevalent worldwide. The primary factors contributing to *H. pylori*-induced gastrointestinal diseases include bacterial motility, adherence, establishment, and a variety of virulence factors. Bacterial outer membrane proteins (OMPs) and flagellar proteins significantly facilitate these processes. Notably, *H. pylori* possess well-characterized OMPs such as *HpaA* and *Omp18*, while *FlaA* and *FlaB* are recognized as the most extensively studied flagellar proteins [9, 13, 14].

H. pylori possess virulence factors, notably the cytotoxic-associated genes (Cag) and the pathogenicity island (PAI), which are critical in eliciting inflammatory responses. Research indicates that strains of H. pylori expressing *CagA* (Cytotoxin-associated antigen A) with high levels of phosphorylation are significantly associated with an increased risk of gastric cancer. These findings underscore the importance of *CagA* in the pathogenesis of H. pylori-related illnesses, particularly its role in promoting chronic inflammation that can lead to malignancy [12, 15, 16]. *OipA* (outer membrane inflammatory protein A) is primarily implicated in the pathogenesis of duodenal ulcers [12, 17, 18]. Human gastric biopsy samples demonstrate the involvement of *OipA* and *CagA* in the pathogenesis of gastric cancer and duodenal ulcers. Both *OipA* and CagA are associated with increased inflammatory responses and higher risks of severe clinical consequences, including peptic ulcer disease and gastric malignancies. Their presence in *H. pylori* strains is associated with significant mucosal inflammation, underscoring their roles as critical virulence factors in *H. pylori*-related diseases [12, 19-21].

The *VacA* (Vacuolating cytotoxin A) produced by H. pylori has profound effects on epithelial cells, aiding in the progression of stomach cancer, particularly in its activated form. The natural immune reaction relies on design recognition receptors, such as *Nod1* (Nucleotide-binding oligomerization domain-containing protein 1), which detect molecules associated with pathogens and are activated by the *CagA* toxin. Additionally, Toll-like receptors (TLRs) play a crucial role in activating pro-inflammatory genes, with H. pylori stimulating these pathways through TLR2 (Toll-like receptor 2), TLR4(Toll-like receptor 4), TLR5(Toll-like receptor 5), and TLR9 (Toll-like receptor 9), leading to increased levels of antimicrobial peptides associated with intestinal cancer [12, 22-26].

Due to their detrimental roles in *H. pylori* infections, proteins such as *VacA* and *CagA* are promising candidates for vaccine development aimed at providing long-term immunity. Despite extensive research, an effective vaccine against *H. pylori* has not yet been developed. However, existing literature regarding the interaction processes between *H. pylori* and human immune responses could inform the creation of a robust

vaccine strategy [12, 27]. Epitopes are specific antigenic regions on pathogens, identified by host immune responses, leading to the activation of humoral or cellular immune responses that provide protection against these pathogens [12, 28]. Antigen-presenting cells (APCs) activate cytotoxic T lymphocytes, which play a crucial role in eliminating infected cells [12, 29]. MHC-bound peptides interact with the surfaces of *H. pylori*-infected cells, facilitating immune recognition and response. This interaction is crucial for the activation of immune pathways that target *H. pylori*, leading to the destruction of infected cells. Understanding these interactions provides insights into the immune mechanisms involved in *H. pylori* infections and their potential implications for vaccine development [12, 30]. Consequently, MHC molecules present a diverse array of high-affinity epitopes. Recent advancements in immune informatics, along with the availability of various tools for epitope vaccine design, have significantly accelerated research efforts aimed at developing innovative vaccine candidates [12, 31]. Methodologies and technologies are increasingly effective in developing precise and stable multi-epitope subunit vaccines. Immune informatics serves as a reliable and timely approach to developing vaccines against severe infections.

Objectives: This research aimed to develop a multi-epitope subunit vaccine for *H. pylori* using immune informatics, highlighting its feasibility and advantages. B and T cell epitopes were designed from various antigenic proteins within the *H. pylori* proteome, helper T lymphocyte (HTL) epitopes were predicted, and the final vaccine was constructed using multiple epitopes. To validate the stability, expression, and immune response of the final vaccine, molecular docking, thermodynamic stability profiling, in silico expression analysis, and agent-based modeling tools were used.

Materials and Methods

Extraction of targeted protein sequences: The total proteome of *H. pylori* strain 26695 (NC_000915) was extracted in FASTA format from the BacMap server [32]. The online server PSORTb (Ver. 3.0.2) was then employed to determine the subcellular localization of proteins [33]. Proteins obtained from PSORTb were analyzed for antigenicity using the VaxiJen server, selecting those with high antigenicity scores for further investigation. Eleven proteins were chosen for vaccine design based on their significance in *H. pylori* infection and their contribution to pathogenicity, including *BabA*(Bloodgroup antigenbinding adhesin A), *SabA*(Sialic acidbinding adhesin A), *HSP* (Heat shock protein), *DupA* (Duodenal ulcer promoting gene A), *FlaA* (Flagellin A) , FlaB (Flagellin B), *CagA*, *OipA*, FecA (Ferric enterobactin receptor A), *UreA* (Urease subunit A), and *VacA*, based on their significance in *H. pylori* infection and their contribution to pathogenicity. Amino acid sequences were retrieved from the UniProt Knowledge Base.

Prediction of immune cell epitopes and human homology: B-cell epitopes were predicted using ABCpred (0.5 threshold, 16-mer filter). Cytotoxic T lymphocyte (CTL) epitopes were predicted via IEDB MHC-I (ANN 4.0), and helper T lymphocyte (HTL) epitopes were predicted via IEDB MHC-II (NN-align). All predicted epitopes were subjected to sequential filtering: (i) IC_{50} < 50 nM (for T cell epitopes), (ii) VaxiJen antigenicity score > 0.4, (iii) non-allergenic (AllerTop), (iv) non-toxic (ToxinPred), and (v) no human homology (BLASTp against full human proteome, E-value ≥ 0.05). Only epitopes meeting all criteria were selected for downstream docking and vaccine construction.

Predicting population coverage: To

evaluate potential vaccine impact, coverage across the worldwide population was assessed utilizing the IEDB Population Coverage tool for the combined analysis of 22 epitopes and their respective 23 alleles. This evaluation indicated an estimated coverage of approximately 96% of the global population (Tables 2-4). Population coverage estimates depend on allele frequency databases and do not account for linkage disequilibrium, HLA haplotype diversity, or inter-individual variability in antigen processing. Therefore, experimental validation remains essential.

Examination of biological characteristics of identified epitopes: The antigenicity, allergenicity, and toxicity of the selected epitopes were evaluated using different computational tools. Antigenicity was predicted via the VaxiJen web server, utilizing a threshold of 0.4 to identify bacterial epitopes based on physicochemical properties in an alignment-independent manner. Allergenicity was assessed using the AllerTop V.2.0 website, while toxicity predictions were performed using ToxinPred, with all parameters set to defaults. Only epitopes predicted to be antigenic, non-toxic, and non-allergenic were retained for subsequent analyses [34].

Molecular docking between T lymphocyte epitopes and MHC alleles: This technique assesses the binding strength of T lymphocyte epitopes to their related major histocompatibility complex (MHC) alleles. The three-dimensional (3D) structures of MHC alleles were sourced from the RCSB PDB database and analyzed with PyMOL software to eliminate unneeded elements. Similarly, the selected epitopes were modeled in 3D structure using the PEP-FOLD 3.5 server, followed by energy minimization with Swiss-PDB Viewer. The docking process was conducted using ClusPro 2.0.

Construction of the vaccine sequence: The mRNA vaccine was meticulously designed from the N-terminus to the C-terminus, incorporating a sequence that includes a 5′ m7GCap, a 5′ UTR, a Kozak sequence, a tPA (Tissue plasminogen activator) signal peptide, an EAAAK linker, an RpfE (Resuscitation promoting factor E) adjuvant, a GPGPG linker, Helper T Lymphocyte (HTL) epitopes, KK and LBL epitopes, an AAY linker, CTL epitopes, a MITD (MHC class I trafficking domain) sequence, a stop codon, a 3′ UTR, and a Poly (A) tail. Three different linkers—AAY, KK, and GPGPG—were utilized to connect the chosen epitopes, providing varying degrees of flexibility and rigidity to ensure proper separation and independent functionality of the domains. The mRNA vaccine was designed for parenteral (intramuscular) administration, which is the standard route for licensed mRNA vaccines (e.g., COVID-19 vaccines). Although this route primarily induces systemic immunity, emerging evidence suggests that parenteral mRNA vaccination could also generate mucosal responses through recirculating B and T cells homing to mucosal sites via integrin expression (e.g., α4β7).

Assessment of the biological features of the designed vaccine: To assess the vaccine's effectiveness, its antigenicity was assessed using two distinct servers: VaxiJen 2.0 and ANTIGENpro. VaxiJen 2.0 relies on physicochemical characteristics of the construct, while ANTIGENpro employs machine learning algorithms based on microarray data. The translated open reading frame (ORF) sequence served as input for the constructed mRNA vaccine. Additionally, allergenicity was assessed through the AllerTOP 2.0 server, and toxicity was predicted using the ToxinPred server. The ProtParam online web server was also used to predict various physicochemical properties of the construct.

In silico immune simulation: To comprehensively evaluate the immune

response to the vaccine construct, an online simulation server known as C-ImmSim was employed. This server simulates immune responses through interactions with epitopes and lymphocyte receptors [35]. The immune response simulation was conducted with default settings over three doses administered within four weeks, consistent with typical vaccination schedules.

Codon adaptation and prediction and validation of secondary and 3D structures: Codon sequences in the vaccine were optimized for efficient expression in human cells using the GenSmart Codon Optimization tool by GenScript. The RNAfold tool from the Vienna RNA Package 2.0 was used to predict the mRNA vaccine secondary structure. ESEfinder was used to check cryptic splice sites. The secondary structure of the peptide sequence was predicted using the PHYRE2 server, which is known for its high accuracy with position-specific scoring matrices. Additionally, three-dimensional structures were predicted using the Robetta server, with validation performed through ProSAweb, PROCHECK, and ERRAT tools.

Vaccine structure flexibility and prediction of conformational B cell epitopes: The structural stability of the vaccine was assessed using CABS Flex 2.0 server simulations to analyze protein dynamics over time [36]. Parameters such as 50 cycles and an overall weight of 1.0 were established for this analysis. Discontinuous B-cell epitopes within the protein's 3D structure were identified using the ElliPro online server, which utilizes geometric features of the model for prediction.

Molecular docking study of the designed vaccine and dynamics simulation: Molecular docking between the 3D structure of the vaccine and toll-like receptors (TLRs) 2, 4, 5, and 9 was conducted using the ClusPro server and the PIPER docking algorithm [34]. To evaluate the physical movements and stability of TLR-vaccine complexes (TLR2-vaccine and TLR4/5/9-vaccine), dynamic simulation analyzes were performed using the iMODS server to visualize atomic movements over time [11].

Findings

Prediction and selection of B-cell epitopes, selection of CTL epitopes, and assessment of HTL epitope: The computational findings indicated that the identified B-cell epitopes, particularly those from *FlaA*, *BabA*, and *DupA*, were promising candidates for further vaccine development research. Their high antigenicity scores, along with computational predictions of low allergenicity and non-toxic properties, indicated a potentially favorable safety profile in silico, making them computationally suitable for immunization strategies; however, experimental validation is required to confirm these predictions (Table 1). Similarly, the identified epitopes from *BabA*, *CagA*, and *FlaA* showed high predicted antigenicity scores and computationally favorable safety profiles, and their association with specific HLA alleles indicated their potential effectiveness across diverse populations, though this remains a theoretical estimate requiring laboratory confirmation (Table 2). Likewise, the predicted MHC class II epitopes from *CagA*, *DupA*, and *FlaA* represented computational candidates for further vaccine development research due to their high predicted immunogenicity scores and favorable safety profiles; their association with specific HLA alleles indicated their theoretical potential efficacy across diverse populations, but in vitro binding assays and in vivo immunogenicity studies are necessary to substantiate these predictions (Table 3). Overlap analysis revealed that three peptides (GDKLDYKRVVSVYLN, SSGLRINKAADDSSG, DIASGTAVRFEPGEEK) functioned as both HTL and B-cell epitopes. Additionally, two

Table 1) Candidate B-cell epitopes and their biological properties in the study

GenBank ID	Protein Name	Peptide	Vaxjen Score	ABCpred Score	AllerTOP	ToxinPred	Human Homology (E-Value)
A0A0A8TSK2	BabA	LSEVKYTYTCSGGGNT	1.7837	0.91	N	N	7.9
AAB58747.1	CagA	QPDIATTTTHIQGLPP	0.9537	0.95	N	N	4.1
PUD42579.1	DupA	GSTGSGKSTFISFLIA	1.6582	0.89	N	N	0.091
A0A7G1HS92	FecA	IPVYMAPYAHIELDIF	1.2220	0.85	N	N	24
AAU21201.1	FlaA	DGRGIEIKTDSVSNGP	2.0041	0.89	N	N	11
TPI06461.1	OipA	GETPRATTDSSSTANL	1.4587	0.94	N	N	30
A0A068LKR0	SabA	SG CATTNSTSNQPSST	1.4591	0.88	N	N	3
AAK69743.1	UreA	DIASGTAVRFEPGEEK	1.4279	0.85	N	N	1.7

Table 2) Studied T lymphocyte epitopes, MHC class I alleles, and their biological properties

GenBank ID	Protein Name	Epitope	Start	End	IEDB Score	VaxiJen	Aller TOP	Toxin Pred	Human Homology (E-Value)	HLA-Allele
A0A0A 8TSK2	*BabA*	AELKYRRLY	8	16	0.985894	1.3304	N	N	8.1	HLA-B*44:03
AAB 58747.1	*CagA*	GINPEWISK SSNKELVGK	30 19	38 27	0.904802 0.909643	1.2858 0.8680	N N	N N	6.5 9	HLA-A*11:01 HLA-A*11:01
PUD 42579.1	*DupA*	MYLFHKLFF	31	39	0.917322	1.1436	N	N	13	HLA-A*24:02
AAU 21201.1	*FlaA*	QVAETTVNLR TTSDKIGQVR	22 24	31 33	0.965311 0.932268	1.4982 1.3575	N N	N N	46 66	HLA-A*68:01 HLA-A*68:01
AAA 25016.1	*FlaB*	HAVGVQNNR KLSSGLRINK	15 31	23 40	0.969152 0.938462	1.3683 1.0862	N N	N N	107 32	HLA-A*68:01 HLA-A*03:01
A0A 068LKR0	*SabA*	RLYSVYLNY	40	48	0.965183	1.2510	N	N	6.1	HLA-A*03:01
AAU 85846.1	*VacA*	NIKNVEITR	60	68	0.903305	1.1799	N	N	26	HLA-A*68:01
P42383	*HSP*	AEDIEGEAL	10	18	0.945834	1.6492	N	N	2.2	HLA-B*40:01
TPI 06461.1	*OipA*	RTLDANTLK	44	52	0.944731	1.6383	N	N	26	HLA-A*11:01

CTL epitopes (RLYSVYLNY, QVAETTVNLR) were found to be nested within larger HTL epitopes, suggesting potential dual presentation pathways.

Investigation of molecular docking of MHC and corresponding T cell epitopes: In this study, 19 lymphocyte epitopes were identified, which could recognize 22 MHC alleles, with some epitopes binding to multiple alleles. The identified CTL epitopes, particularly those with high binding affinities like RLYSVYLNY and MYLFHKLFF, represented promising computational candidates for inclusion in vaccine formulations aimed at enhancing CTL responses against intracellular pathogens. The ability to present these peptides across multiple HLA alleles could improve vaccine efficacy in diverse populations. In summary, the analysis of CTL epitopes revealed

Table 3) Studied T lymphocyte epitopes, MHC class II alleles, and their biological properties

GenBank	Proteins	Peptide MHCII	Start	End	Score IEBD	Vaxijen	Aller	Toxin	Homo Sapiens Homology (E-Value)	Allele
AAB 58747.1	*CagA*	NEPIYAKVNKKKTGQ	49	63	0.9358	0.9017	N	N	14	HLA-DRB1*11:01
PUD 42579.1	*DupA*	KFMLNIDSDNQQDNK	71	85	0.9490	1.5719	N	N	2.5	HLA-DRB1*04:01
A0A 7G1HS92	*FecA*	SRAYSGISNSAAGGY SEQDYKINRFANLRP	69 122	83 136	0.9494 0.8819	0.8836 0.9948	N N	N N	14 35	HLA-DRB1*04:01 HLA-DPA1*01:03
AAU 21201.1	*FlaA*	LRINKAADD	31	40	0.8982	1.0523	N	N	13	HLA-DRB3*02:02
AAA 25016.1	*FlaB*	SSGLRINKAADDSSG EFQIGAYSNTTVKAS	33 76	47 90	0.8914 0.9636	1.5970 1.2078	N N	N N	20 97	HLA-DRB3*02:02 HLA-DRB1*15:01
TPI 06461.1	*OipA*	GDKLDYKRVVSVYLN	4	18	0.8449	0.9145	N	N	7.1	HLA-DRB1*07:01
A0A 068LKR0	*SabA*	VYNLKSNQANIVATY	387	401	0.9154	0.8448	N	N	41	HLA-DRB3*02:02
AAK 69743.1	*UreA*	RLDIASGTAVRFEPG	25	39	0.8619	1.5447	N	N	1.5	HLA-DQA1*05:01/ DQB1*03:01

Table 4) Docking analysis results of CTL epitopes with corresponding MHC alleles

Type of T Lymphocyte	Epitope	MHC Alleles	PDB ID of MHC Allele	Binding Affinity
CTL	MYLFHKLFF	HLA-A*24:02	4U6X	-860.4
	AELKYRRLY	HLA-B*44:03	3KPN	-679.1
	GINPEWISK	HLA-A*11:01	5WJN	-575.2
	QVAETTVNLR	HLA-A*68:01	6PBH	-735.0
	RLYSVYLNY	HLA-A*03:01	7L1C	-860.6
	AEDIEGEAL	HLA-B*40:01	6IEX	-567.5

Table 5) Docking analysis results of HTL epitopes with corresponding MHC alleles

Type of T Lymphocyte	Epitope	MHC Alleles	PDB ID of MHC Allele	Binding Affinity
HTL	KFMLNIDSDNQQDNK	HLA-DRB1*04:01	5NI9	-716.5
	EFQVGAYSNQSIKAS	HLA-DRB1*15:01	8TBP	-705.2
	HAVGVQNNR	HLA-DRB3*02:02	2Q6W	-627.5
	AMGFALAVVHPAAGN	HLA-DRB1*09:01	6BIY	-769.1
	GDKLDYKRVVSVYLN	HLA-DRB1*07:01	7Z0Q	-799.3

significant computational insights into their binding affinities and their potential to elicit immune responses. High-affinity peptides are likely to be effective in activating CTLs when presented by their respective MHC class I molecules. Future research should focus on experimental validation of these predictions and exploration of their immunogenicity in clinical settings. Understanding the interplay between epitope binding affinity, HLA diversity, and T cell responses will be essential for optimizing vaccine strategies tailored to various populations (Table 4). The identified HTL epitopes, particularly those with high binding affinities like GDKLDYKRVVSVYLN and AMGFALAVVHPAAGN, represented promising candidates for inclusion in vaccine formulations aimed at enhancing HTL responses against pathogens. The ability to present these peptides across multiple HLA alleles could improve vaccine efficacy in diverse populations. In conclusion, the analysis of HTL epitopes revealed significant insights into their binding affinities and their potential to elicit immune responses. High-affinity peptides are likely to be effective in activating HTLs when presented by their respective MHC class II molecules (Table 5). In this study, eight epitopes were selected based on our initial analysis, and molecular docking studies were conducted with their corresponding MHC alleles, utilizing crystallographic structures acquired from the RCSB Protein Data Bank (PDB). The binding affinities were predicted using ClusPro 2.0, and the results are summarized in Table 5. Among these epitopes, LSDGAAAGY demonstrated the highest binding affinity for its corresponding MHC allele (HLA-A*01:01), with a value of -643.6 kcal /moL. The molecular docking analysis revealed that this epitope was optimally positioned within the binding cleft of its associated MHC allele (Figure 1). The vaccine construct design comprised several components arranged in a specific sequence. Below is a detailed breakdown of each component:

The mRNA vaccine construct was proposed from the N- to C-terminus as follows: 5′ m7GCap– 5′ UTR–Kozak sequence–signal peptide (tPA)–EAAAK linker- adjuvant (RpfE)–GPGPG- SEQDYKINRFANLRP - GPGPG– KFMLNIDSDNQQDNK –GPGPG– SRAYSGISNSAAGGY –GPGPG - NEPIYAKVNKKKTGQ – GPGPG– EFQVGAYSNQSIKAS –GPGPG– LRINKAADD - GPGPG– SSGLRINKAADDSSG –GPGPG -GDKLDYKRVVSVYLN –GPGPG– VYNLKSNQANIVATY –GPGPG - RLDIASGTAVRFEPG -KK - LSEVKYTYTCSGGGNT–KK-QPDIATTTTHIQGLPP–KK-GSTGSGKSTFISFLIA–KK-IPVYMAPYAHIELDIF–KK-DGRGIEIKTDSVSNGP–KK-GETPRATTDSSSTANL-KK-SGCATTNSTSNQPSST- KK-DIASGTAVRFEPGEEK- AAY-AELKYRRLY-AAY RLYSVYLNY- AAY -SSNKELVGK- AAY - GINPEWISK-AAY - MYLFHKLFF- AAY - QVAETTVNLR- AAY - TTSDKIGQVR- AAY - HAVGVQNNR- AAY - RTLDANTLK- AAY - KLSSGLRINK- AAY - AEDIEGEAL- AAY L-IKNVEITR- AAY -MITD sequence–Stop codon–3′ UTR–Poly (A) tail.

Inspection of the designed vaccine biological properties and population coverage: The designed vaccine was evaluated for its antigenicity, allergenicity, toxicity, and physicochemical properties using a range of computational tools, including VaxiJen, ANTIGENpro, AllerTop, ToxinPred, and the ProtParam server. According to the analysis results, the vaccine exhibited favorable antigenic properties and was both non-toxic and non-allergenic. Furthermore, the physicochemical analysis revealed that the vaccine was thermally stable and hydrophilic, with a grand average of hydropathicity (GRAVY) score of -0.616 (Table 6). These findings suggest that the designed mRNA vaccine has good potential as a candidate for further

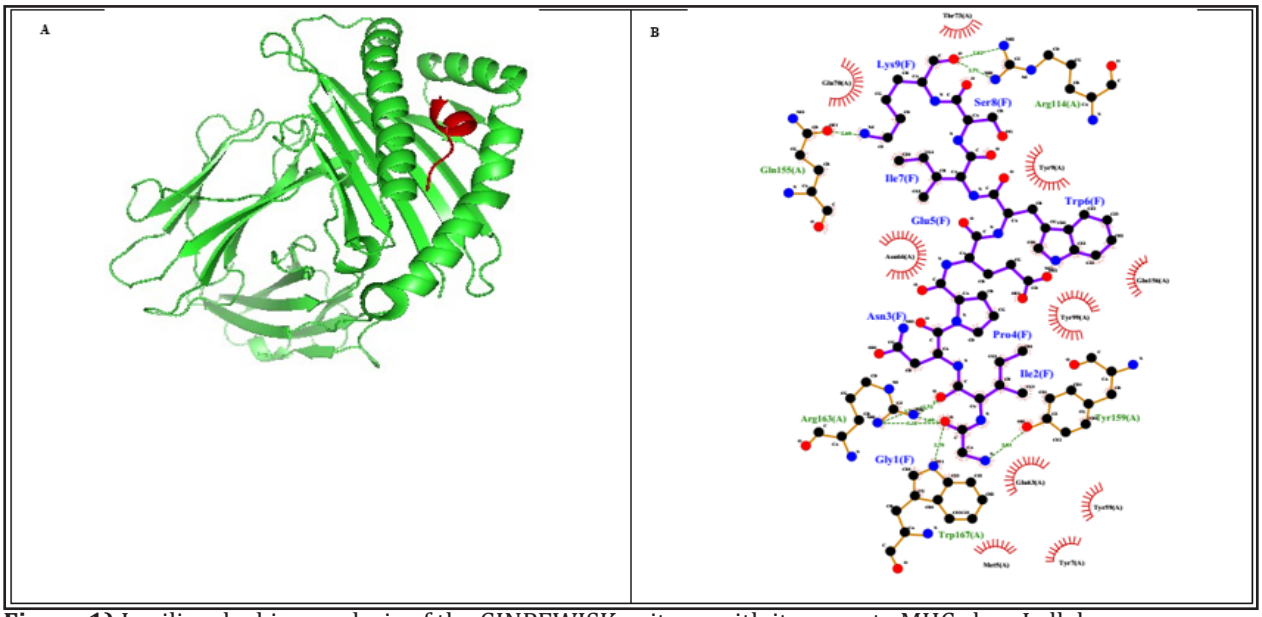


Figure 1) In silico docking analysis of the GINPEWISK epitope with its cognate MHC class I allele, HLA-A*11:01. (A) Three-dimensional ribbon representation of the peptide–MHC complex, visualized using PyMol. (B) Two-dimensional interaction diagram depicting hydrogen bonds and hydrophobic contacts at the binding interface, generated using LigPlot+.

Table 6) Physicochemical characteristics of the designed mRNA vaccine

Property	Measurement	Indication
Total number of amino acids	479	Appropriate
Molecular weight	50843.03	Appropriate
Formula	C2248H3546N636O700S5	-
Theoretical pI	9.65	Acidic
Total number of negatively charged residues (Asp + Glu)	39	-
Total number of positively charged residues (Arg + Lys)	65	-
Total number of atoms	7135	-
Instability index (II)	32.33	Stable
Aliphatic index (AI)	65.30	Thermostable
Grand average of hydropathicity (GRAVY)	-0.616	Hydrophilic
Antigenicity (using VaxiJen)	1.1603	Antigenic
Antigenicity (using ANTIGENpro)	0.936101	Antigenic
Allergenicity (using AllerTop 2.0)	Non-allergenic	Non-allergenic
Toxicity (ToxinPred)	Non-toxic	Non-toxic

development. The analysis of the vaccine efficacy using the Immune Epitope Database (IEDB) tool indicated a high estimated coverage of 96.09% globally. This finding underscores the vaccine's potential to elicit immune responses across diverse populations, which is a critical factor in vaccine development.

In silico assessment of the immune responses to the final construc: The analysis of the immune responses following the administration of three doses of the vaccine revealed significant computational insights into its efficacy and potential for long-term immunity. The results (Figure 2) indicated that both the second and

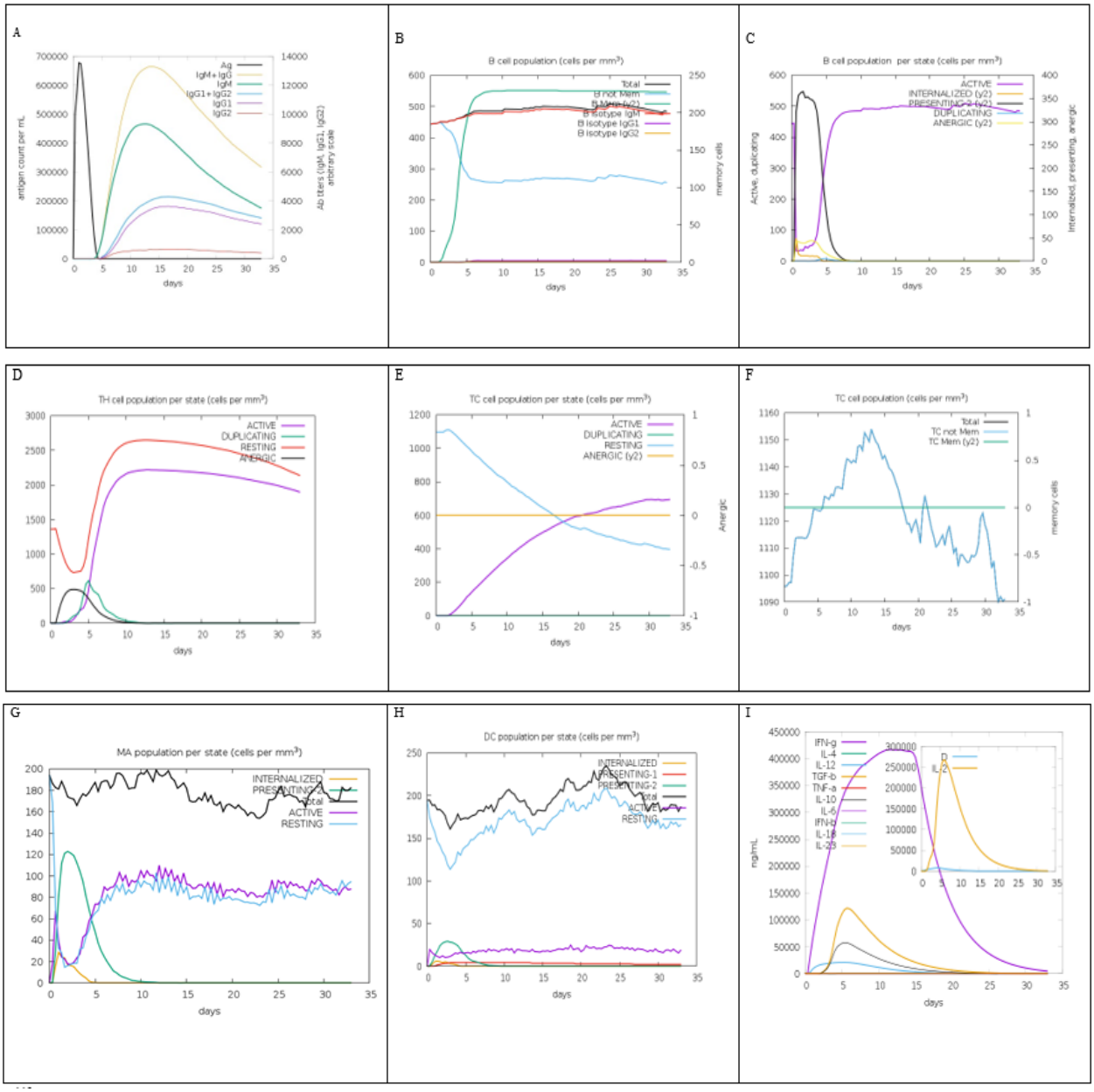


Figure 2) In silico time-course immune responses elicited by the mRNA vaccine construct, as simulated by the C-ImmSim server. (A) Kinetics of serum immunoglobulin (IgM, IgG, and total Ig) production following antigen administration. (B) Dynamics of the total B-cell population. (C) Helper T-lymphocyte (HTL) population dynamics, and (D) their distribution according to activation states (e.g., resting, active, and memory). (E) Cytotoxic T-lymphocyte (CTL) population kinetics over time. (F) Epithelial cell population dynamics, (G) macrophage population, and (H) dendritic cell population. (I) Cytokine and interleukin secretion profiles, along with the calculated Simpson's diversity index (D), indicating the breadth and heterogeneity of the simulated immune response.

third doses stimulated significantly higher immune responses compared to the initial dose. Notably, immunoglobulin M (IgM) levels exceeded those of immunoglobulin G (IgG), suggesting an early immune response characterized by IgM production, which is typically associated with initial exposure to an antigen. The predicted elevation of immunoglobulin levels following antigen exposure points to the development of immune memory and trained immunity. The observation of isotype switching, where B cells switch from producing IgM to IgG, alongside the formation of B cell memory,

indicates a robust adaptive immune response capable of responding more effectively to subsequent antigen exposures. The presence of memory T cells suggests that the vaccine not only induces an immediate immune response but also establishes long-term immunological memory, which is vital for effective protection against future infections. Further evidence of heightened macrophage activity indicates enhanced innate immunity, which plays a critical role in pathogen clearance and shaping adaptive responses. The consistent activity of dendritic cells suggests effective antigen presentation and stimulation of T cell responses, reinforcing the overall efficacy of the vaccine. The elevated levels of interferon-gamma (IFN-γ) and interleukin-2 (IL-2) are particularly noteworthy, as these cytokines are key indicators of T cell activation and proliferation. IFN-γ is essential for enhancing macrophage function and promoting Th1-type immune responses, while IL-2 is crucial for T cell growth and differentiation. The increase in epithelial cells contributing to innate immunity further underscores the vaccine's potential to bolster both innate and adaptive immune mechanisms. Importantly, the application of Simpson's index (D) to assess diversity within immune responses indicated a distinct and varied immune response. This metric could provide insights into the robustness and breadth of the immune responses elicited by the vaccine, suggesting that it may effectively target multiple epitopes or pathways. In summary, the administration of three doses of the vaccine demonstrated a strong and sustained immune response characterized by elevated antibody levels, increased CTL and HTL populations, enhanced macrophage activity, and significant cytokine production. These findings support the potential for long-term immunity and highlight the importance of multiple doses in achieving an effective immunological profile.

Optimization of codon usage for the constructed mRNA vaccine: Codon optimization tools are essential for enhancing the translation efficiency of mRNA vaccines after entry into host cells. In this study, the GenSmart (GS) Codon Optimization tool was used to facilitate effective vaccine expression into human cells. The mRNA coding sequence (CDS) was determined to be 1,896 nucleotides in length. To evaluate the quality of the optimized construct, the GS Rare Codon Analysis tool was employed. The calculated codon adaptation index (CAI) value was 0.95 (Fig. 3A), which exceeds the acceptable threshold of 0.95, indicating that the construct is suitable for expression. The optimal GC content for efficient expression in human hosts typically ranges from 30 to 70%. The optimized construct achieved an average GC content of 66.78% (Fig. 3B), aligning well within this recommended range. Additionally, the codon frequency distribution (CFD) was recorded at 0% (Fig. 3C), suggesting that there were no rare codons that could impede translation efficiency or function; codons with a frequency below 30% may negatively affect the translational machinery.

Modeling the secondary structure of the mRNA vaccine: The mRNA vaccine structure was predicted using the RNAfold server, facilitating the assessment of the free energies associated with the predicted structures. The optimized codons of the construct were used as input for this analysis. According to the findings, the mRNA is expected to exhibit stability, characterized by a minimum free energy (MFE) of -449.70 kcal/moL for the primary structure (Fig. 4D) and an MFE of -351.30 kcal/moL for the secondary centroid structure (Fig. 3E). These results suggest that the optimized mRNA construct is likely to maintain structural integrity during synthesis and subsequent cellular processes.

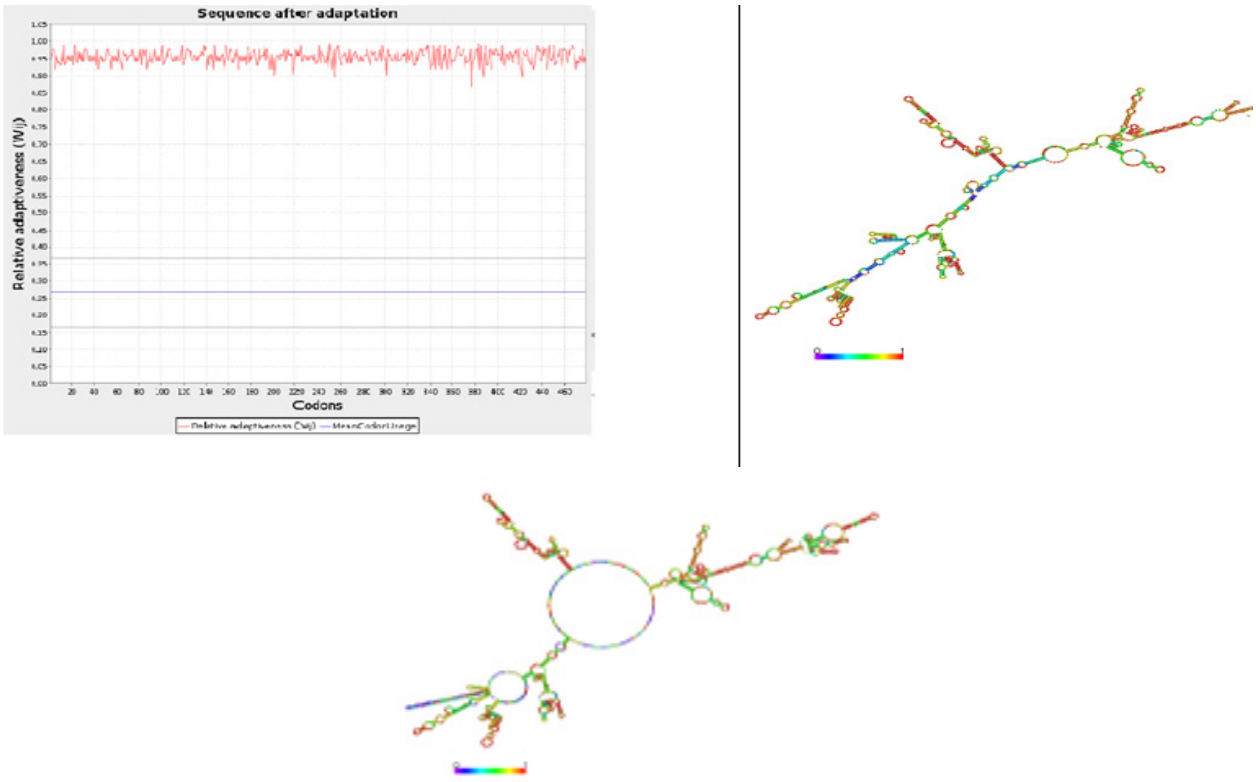


Figure 3) Codon optimization and secondary structure modeling of the designed mRNA vaccine construct, as predicted by the RNAfold web server. (A) Codon Adaptation Index (CAI) value, indicating the translational efficiency of the optimized sequence. (B) The minimum free energy (MFE) secondary structure, representing the most thermodynamically stable folding conformation. (C) The centroid secondary structure, derived from the Boltzmann ensemble of all possible folds, representing the structure with the maximum base-pair probability.

Molecular modeling, evaluation of conformational structures in the designed construct and vaccine 3D structure flexibility: The vaccine secondary structure was predicted using the PHYRE2 web service, which revealed a predominance of alpha helices (Figure 4A). Additionally, the tertiary structure of the peptide was modeled using the Robetta server (Fig. 4B). To assess the stereochemical accuracy of the predicted structure, the PROCHECK server was employed, evaluating both the geometry of individual residues and the overall conformation. The Ramachandran plot generated by PROCHECK (Fig. 5C) indicated that approximately 82.3% of the residues were located in the most favored regions, 15.4% in the additionally allowed regions, and 1.3% in the generously allowed regions. The overall quality factor for the model was calculated to be 88.286. Furthermore, analysis using ProSA-web yielded a negative Z-score of -7.15, suggesting that the 3D protein model is highly consistent (Fig. 4C). These results collectively support the structural integrity and reliability of the predicted vaccine model. Flexibility simulations of protein structures were conducted using the CABS-flex 2.0 web server (Figure 5). This tool facilitates rapid assessments of protein dynamics and conformational flexibility.

Discontinuous B-cell epitopes and molecular docking of the designed vaccine and TLR: The ElliPro server was utilized to predict epitopes, resulting in the identification of five conformational B-cell epitopes. The analysis revealed a total of 197 residues with prediction scores ranging from 0.537 to 0.855. The two-dimensional (2D) and three-dimensional (3D) models of the

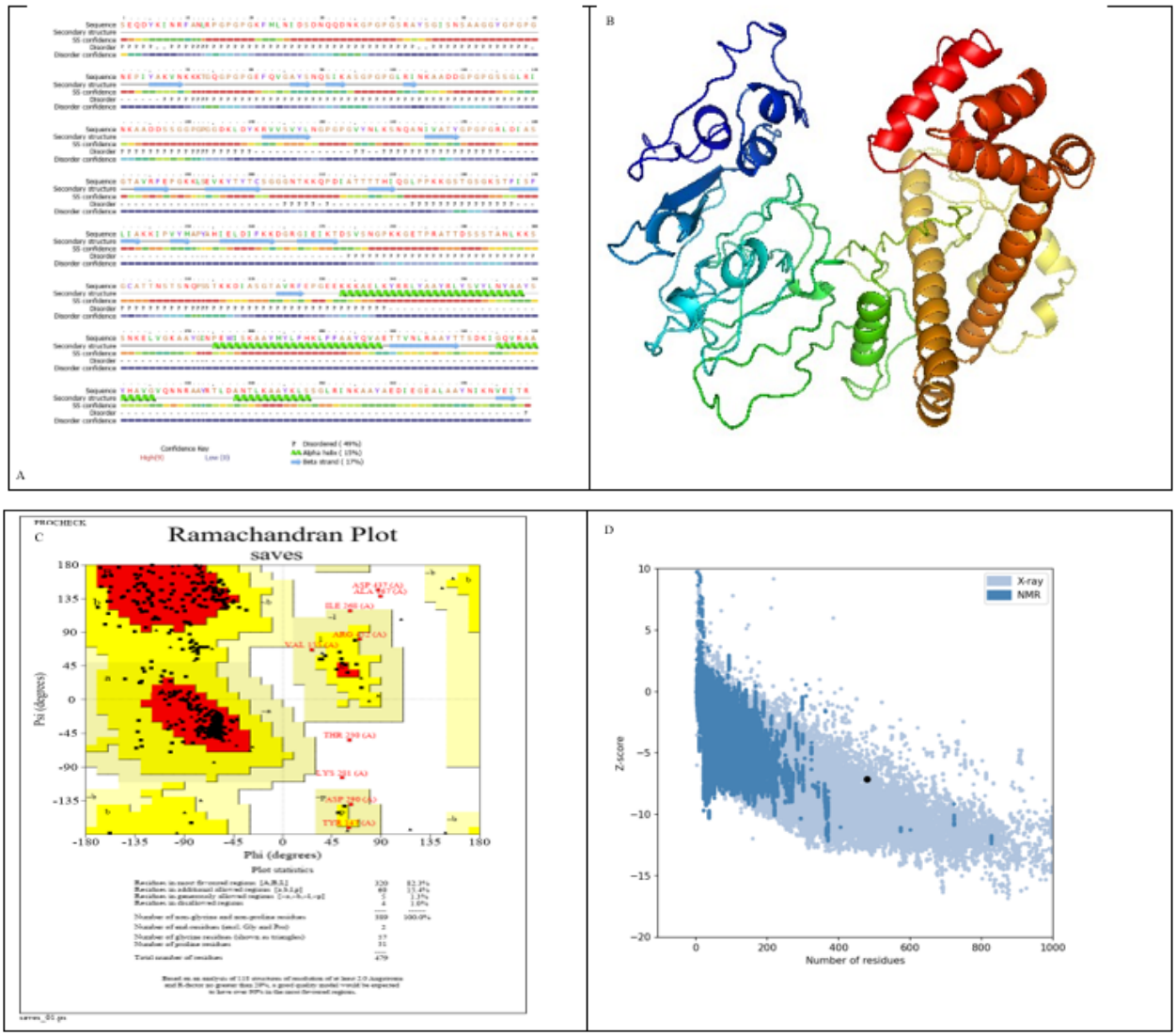


Figure 4) Structural prediction and quality validation of the designed vaccine construct. (A) Secondary structure topology (α-helices, β-strands, and random coils) predicted using the PSIPRED server. (B) Three-dimensional (3D) homology model of the protein construct generated by the Robetta server. (C) Ramachandran plot displaying the distribution of backbone φ/ψ dihedral angles, used to assess the stereochemical quality of the model. (D) ProSA-web Z-score plot, evaluating the overall model quality and fold compatibility.

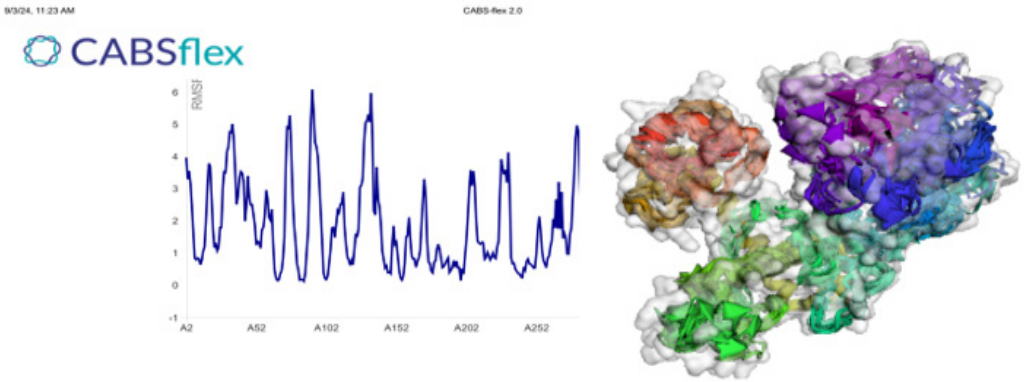


Figure 5) Root-mean-square fluctuation (RMSF) profile of the designed protein vaccine construct, derived from molecular dynamics simulation/normal mode analysis.

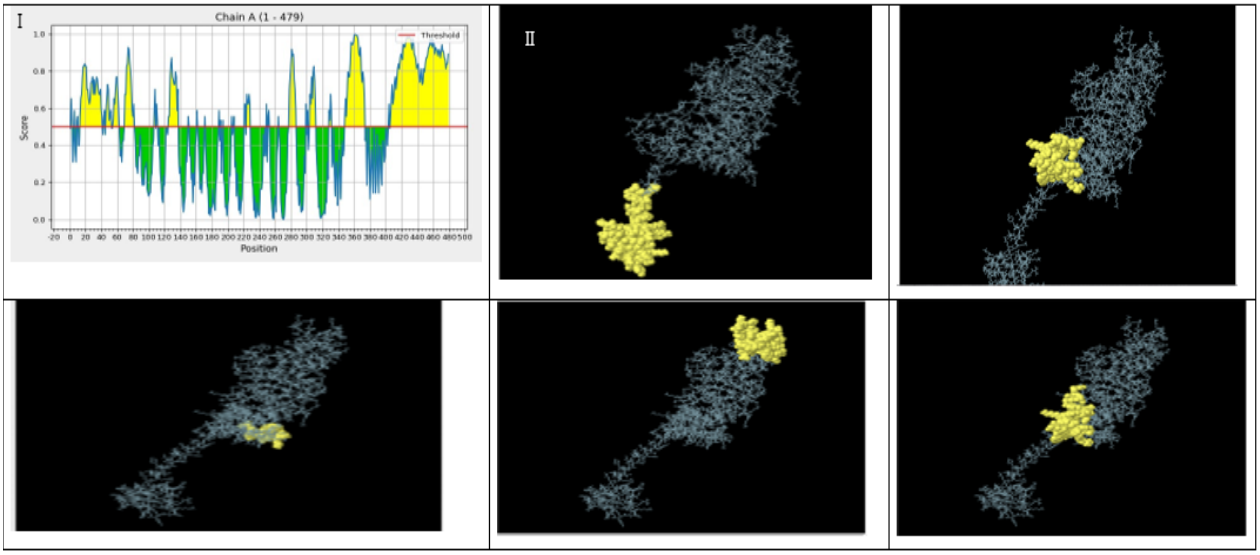


Figure 6) Conformational (discontinuous) B-cell epitopes predicted within the designed vaccine construct using the ElliPro server. (I) Two-dimensional (2D) surface representation illustrating the spatial distribution and residue composition of the five identified epitopes. (II) Three-dimensional (3D) ribbon/surface models displaying the topographical localization of these epitopes on the vaccine tertiary structure.

identified conformational B-cell epitopes are illustrated in Figure 6 (I and II). Molecular docking studies were conducted to evaluate the potential interactions of the vaccine with toll-like receptors 4 (TLR-4) and 2, 5, and 9 using the ClusPro server (Fig. 7A, Fig. 8A, Fig. 9A, and Fig. 10A). Additionally, the detailed interactions between the designed vaccine amino acids and TLR-4 (Fig. 7G) as well as TLR-2, 5, and 9 receptors were analyzed (Fig. 8G, Fig. 9G, and Fig. 10G) utilizing the PDBsum server and LigPlot software.

Molecular dynamics: Molecular dynamics simulations of the vaccine-TLR2, TLR4, TLR5, and TLR9 complexes were conducted using the iMODS platform to evaluate receptor-ligand interactions and investigate conformational dynamics. The summits in the deformation curves (Figures 7B, 8B, 9B, and 10B) indicated deformable loci within the complexes, while twisted amino acids were represented on the conformational curves. The results revealed low deformation rates across all complexes (TLR2: 1.45e-06, TLR4: 1.89e-06, TLR5: 2.12e-06, TLR9: 1.67e-06 AU), indicating higher stability and rigidity. Normal mode analysis (RMA) was performed to characterize protein flexibility, assessing the relationship between RMA results and PDB regions of the docked complexes as depicted in B-factor plots (Figures 7C, 8C, 9C, 10C). RMSF analysis (Supplementary Figure S1 and Table 1) revealed that the vaccine construct exhibited overall low flexibility, with a minimum RMSF value of 0.085 nm (0.85 Å) at residue 143 and an average RMSF value of approximately 0.13–0.16 nm (1.3–1.6 Å) across core structural regions (residues 100–200 and 250–350). Higher flexibility was observed in specific loop regions and near the C-terminus, with peak RMSF values reaching 0.391 nm (3.91 Å) at residue 471, consistent with expected terminal dynamics. The eigenvalues (TLR2: 3.45e-05, TLR4: 2.89e-05, TLR5: 4.12e-05, TLR9: 3.78e-05) were comparable to stable protein-ligand complexes reported in literature, indicating favorable collective motions. Specific values for the complexes are presented in Figures 7D, 8D, 9D, and 10D. Figures 7E, 8E, 9E, 10E indicate covariance matrices illustrating connectivity between amino acid pairs in dynamic regions: red indicates positively correlated residues,

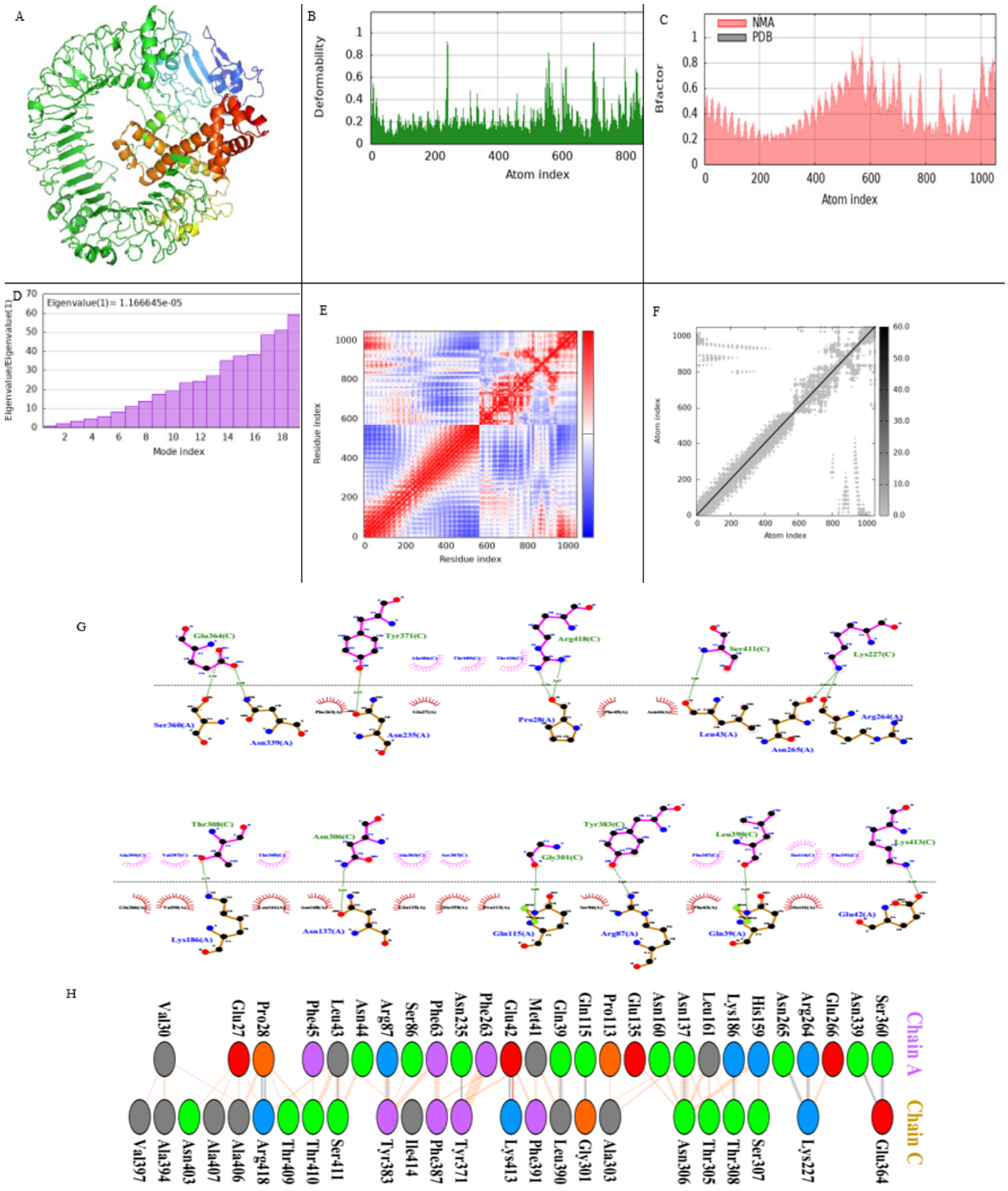


Figure 7) Normal mode analysis (NMA) and molecular dynamics simulation of the vaccine construct–TLR4 complex. (A) Ribbon representation of the docked complex, generated by the ClusPro server. (B) Deformability profile, indicating the intrinsic flexibility of individual residues along the sequence. (C) B-factor plot comparing the computed atomic displacement parameters with theoretical values. (D) Eigenvalue associated with the complex, reflecting the overall stiffness and collective motion of the system. (E) Covariance matrix illustrating correlated (red) and anti-correlated (white) motions between residue pairs. (F) Elastic network model depicting the connectivity and rigidity of the complex backbone, calculated using the iMODS server. (G) LigPlot+ two-dimensional interaction diagram detailing hydrogen bonds and hydrophobic contacts at the receptor–ligand interface. (H) PDBsum-derived schematic of the intermolecular interactions stabilizing the complex.

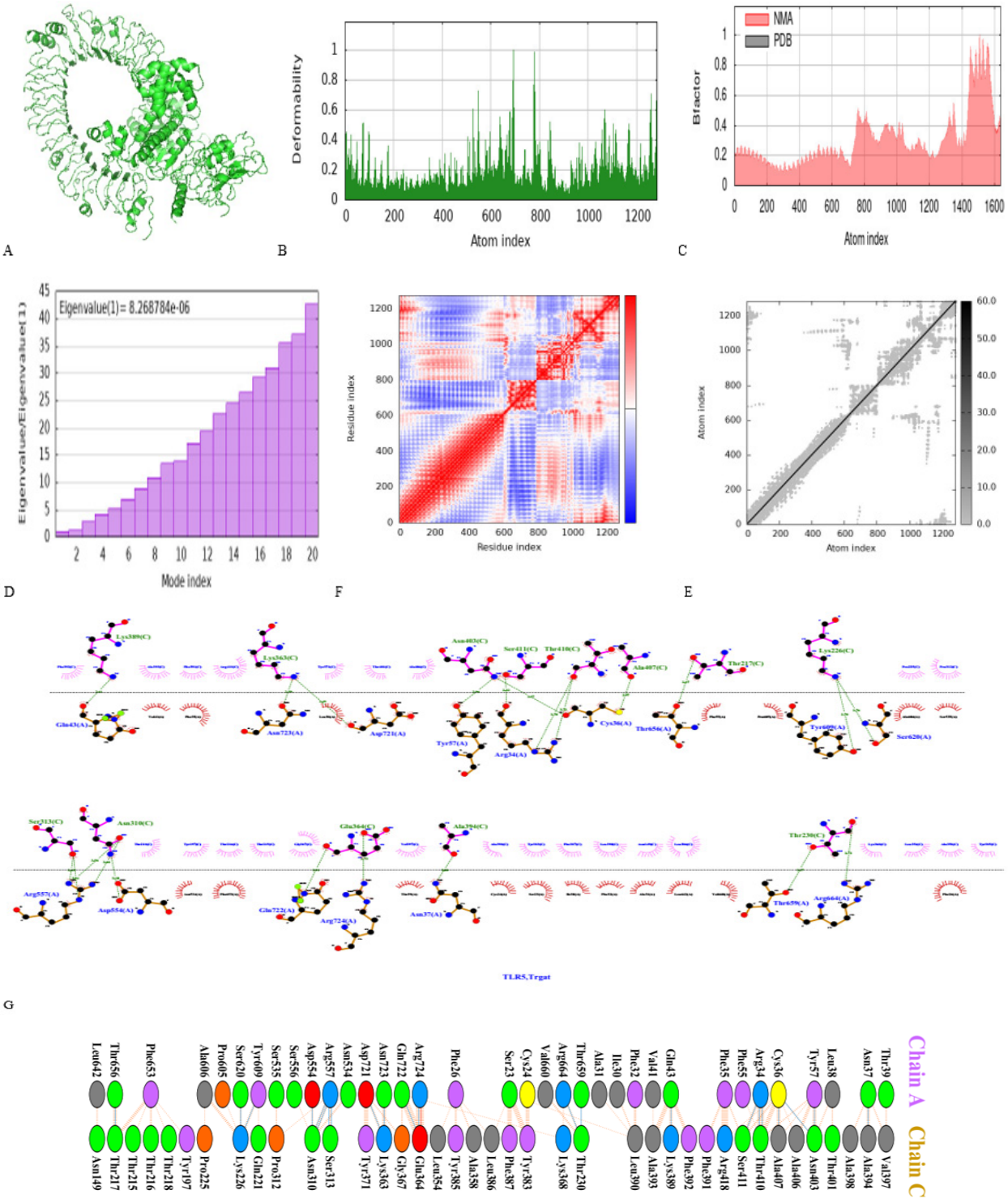


Figure 8) Normal mode analysis (NMA) and molecular dynamics simulation of the vaccine construct–TLR5 complex. (A) Ribbon representation of the docked complex, generated by the ClusPro server. (B) Deformability profile, indicating the intrinsic flexibility of individual residues along the sequence. (C) B factor plot comparing the computed atomic displacement parameters with theoretical values. (D) Eigenvalue associated with the complex, reflecting the overall stiffness and collective motion of the system. (E) Covariance matrix illustrating correlated (red) and anti correlated (white) motions between residue pairs. (F) Elastic network model depicting the connectivity and rigidity of the complex backbone, calculated using the iMODS server. (G) LigPlot+ two dimensional interaction diagram detailing hydrogen bonds and hydrophobic contacts at the receptor–ligand interface. (H) PDBsum derived schematic of the intermolecular interactions stabilizing the complex.

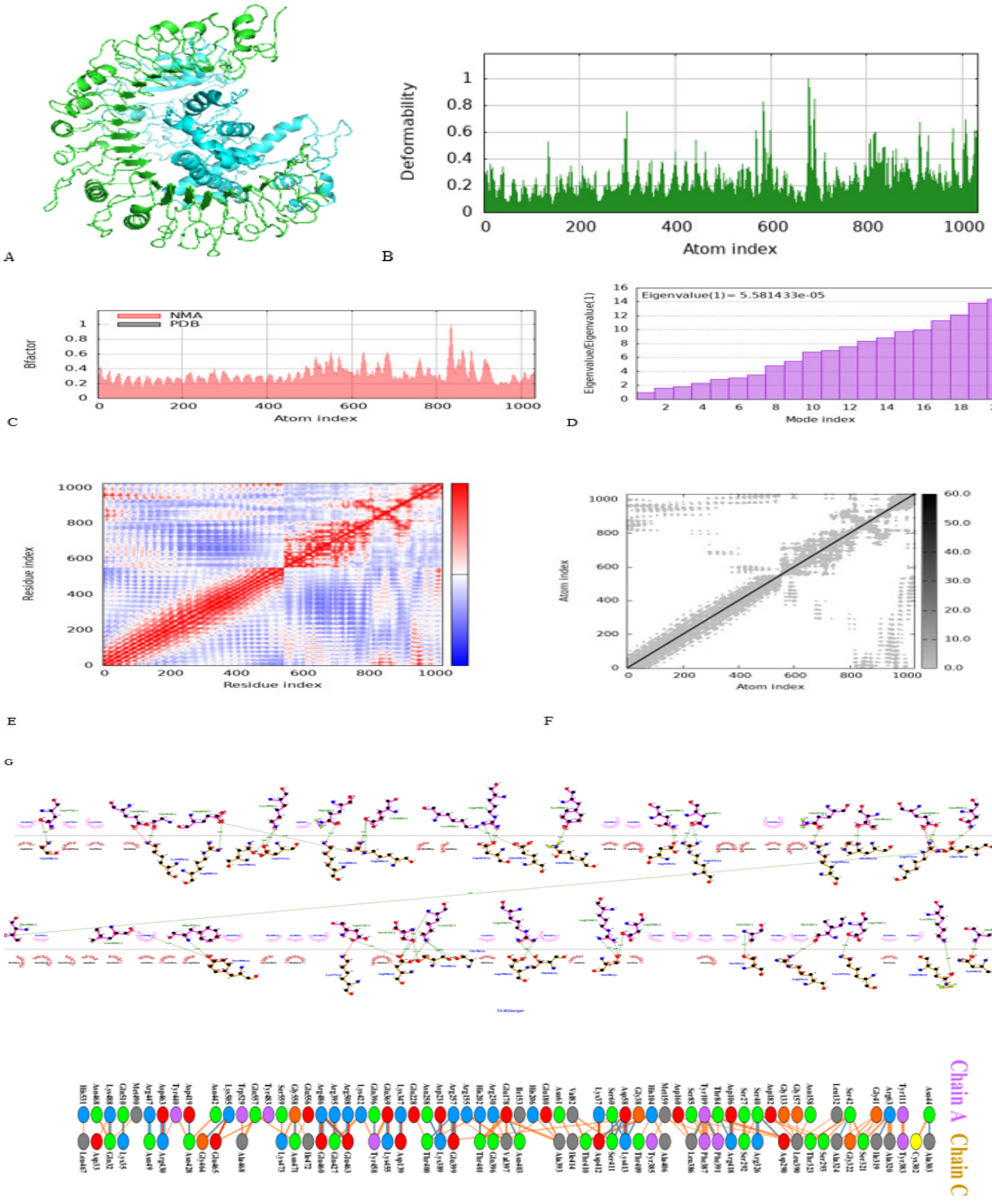


Figure 9) Normal mode analysis (NMA) and molecular dynamics simulation of the vaccine construct–TLR2 complex. (A) Ribbon representation of the docked complex, generated by the ClusPro server. (B) Deformability profile, indicating the intrinsic flexibility of individual residues along the sequence. (C) B factor plot comparing the computed atomic displacement parameters with theoretical values. (D) Eigenvalue associated with the complex, reflecting the overall stiffness and collective motion of the system. (E) Covariance matrix illustrating correlated (red) and anti correlated (white) motions between residue pairs. (F) Elastic network model depicting the connectivity and rigidity of the complex backbone, calculated using the iMODS server. (G) LigPlot+ two dimensional interaction diagram detailing hydrogen bonds and hydrophobic contacts at the receptor–ligand interface. (H) PDBsum derived schematic of the intermolecular interactions stabilizing the complex.

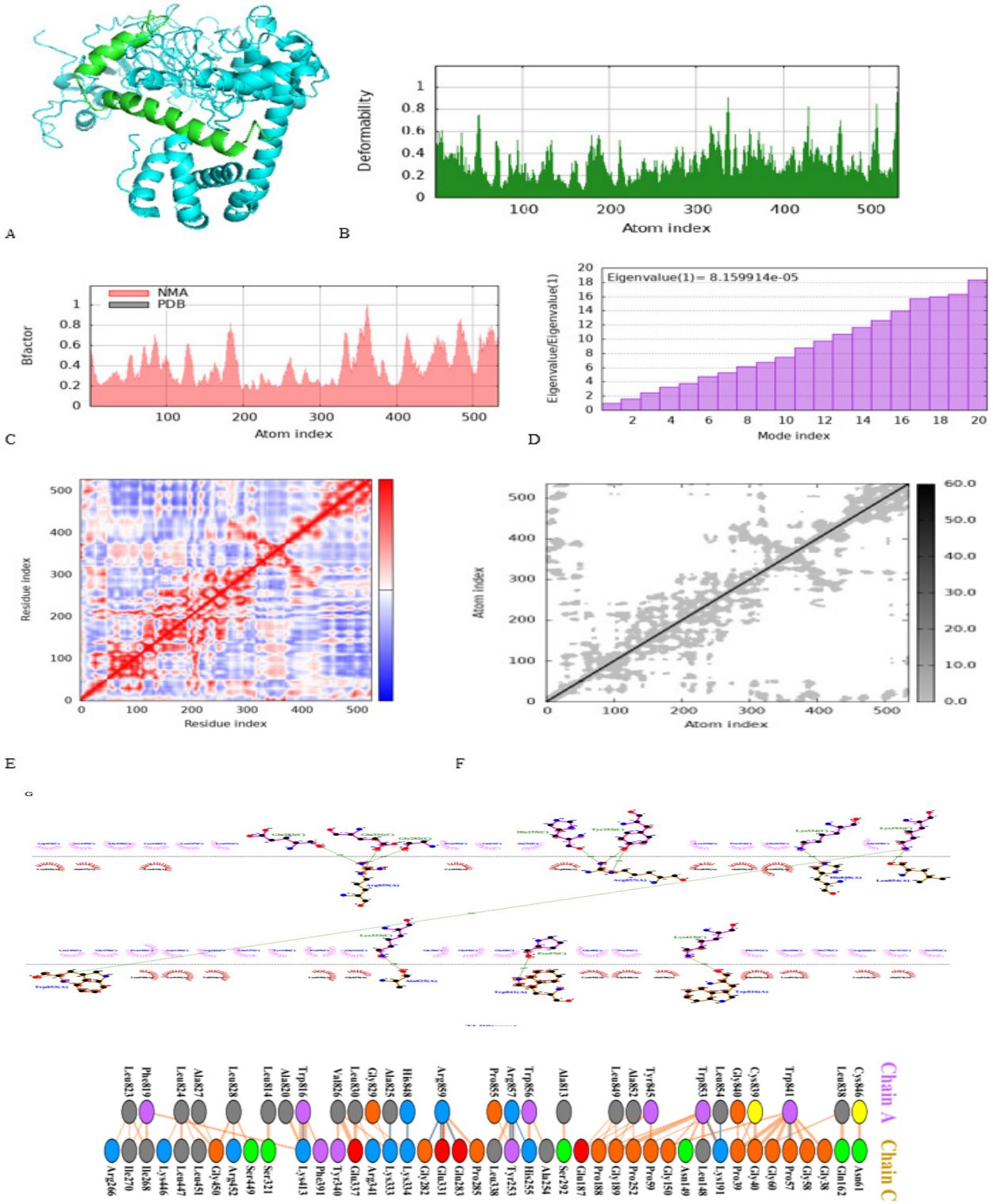


Figure 10) Normal mode analysis (NMA) and molecular dynamics simulation of the vaccine construct–TLR9 complex. (A) Ribbon representation of the docked complex, generated by the ClusPro server. (B) Deformability profile, indicating the intrinsic flexibility of individual residues along the sequence. (C) B factor plot comparing the computed atomic displacement parameters with theoretical values. (D) Eigenvalue associated with the complex, reflecting the overall stiffness and collective motion of the system. (E) Covariance matrix illustrating correlated (red) and anti correlated (white) motions between residue pairs. (F) Elastic network model depicting the connectivity and rigidity of the complex backbone, calculated using the iMODS server. (G) LigPlot+ two dimensional interaction diagram detailing hydrogen bonds and hydrophobic contacts at the receptor–ligand interface. (H) PDBsum derived schematic of the intermolecular interactions stabilizing the complex.

white denotes anti-correlated pairs, and blue signifies uncorrelated residues. Additionally, Figures 7F, 8F, 9F, and 10F show coupling matrices representing elastic network models. Each chain within the complexes displays high immobility, with darker gray regions indicating stiffer areas.

Discussion

H. pylori infection is rapidly spreading in both emerging and developed countries, leading to serious gastrointestinal issues such as persistent gastritis, multifocal atrophic gastritis, gastric dysplasia, and an increased risk of gastric cancer [11]. A critical consideration for *H. pylori* vaccinology is the gastric mucosal environment. Unlike systemic pathogens, *H. pylori* colonizes the gastric epithelium without deep invasion, suggesting that mucosal secretory IgA (sIgA) may be more critical than systemic IgG for preventing initial colonization. The designed mRNA vaccine, intended for parenteral (intramuscular) administration, is expected to elicit strong systemic IgG and T cell responses but only limited direct mucosal IgA production; however, its ability to generate mucosal responses remains computationally unverified. Although this limitation is not insurmountable, studies have shown that systemic vaccination could induce "mucosal homing" of antigen-specific B and T cells via upregulation of CCR9 and α4β7 integrin, leading to measurable IgA in gastric secretions. Furthermore, the distinction between prophylactic (preventing colonization) and therapeutic (clearing established infection) vaccination is paramount; the present design targets conserved virulence factors and could theoretically function in both contexts, but therapeutic application faces additional challenges including immune evasion and established bacterial biofilms. It is explicitly acknowledged that an oral or intranasal mRNA vaccine formulation (e.g., using lipid nanoparticles optimized for mucosal delivery) would be theoretically superior for generating local immunity. The current design represents a first-generation systemic candidate; future iterations should explore mucosal delivery platforms. These limitations are explicitly acknowledged as requiring experimental investigation. Previous attempts at *H. pylori* vaccination have encountered the paradoxical risk of vaccine-enhanced inflammation, where immunization against bacterial antigens exacerbates gastric pathology rather than inducing protection. This is particularly important for antigens like *CagA* and *VacA*, which are directly involved in epithelial damage. Our multi-epitope vaccine design deliberately excludes known toxic domains of these proteins and instead uses short, conserved, non-toxic epitopes. Nonetheless, in silico predictions could not rule out immunopathology, and any future in vivo study must monitor gastric inflammation scores alongside protection.

Reverse vaccination technology has emerged as an innovative strategy for developing subunit vaccines, providing improved safety and efficacy compared to traditional approaches that typically require greater expenses and longer development times. Advances in microbial genomics and proteomics have facilitated the screening and evaluation of vaccine antigens, thereby improving targeted vaccine design and response to new infectious diseases [35]. Although antibiotic treatment for infectious diseases is expensive and contributes to microbial resistance, vaccination presents an effective preventive measure. Classical vaccination methods have led to the development of advanced subunit vaccines composed of particular pathogenic protein sequences that effectively stimulate immune responses. For a subunit vaccine against *H.*

pylori, key virulence factors such as *CagA*, *HSP*, *VacA*, *SabA*, *DupA*, *OipA*, *UreA*, *FlaA*, *FecA*, and *BabA* were identified using online resources to guarantee a strong vaccine design [12]. Studies have demonstrated the effectiveness of mRNA vaccines in eliciting HTL and CTL responses against various pathogens, including *H. pylori*, emphasizing the potential of mRNA technology for vaccine development [37]. CTLs directly target and eliminate infected cells, whereas HTLs coordinate and direct immune responses, making mRNA vaccines viable candidates for targeted vaccination against *H. pylori* infections. However, further inquiry is necessary to evaluate the efficacy and safety of mRNA vaccines in larger populations over longer durations. Identifying epitopes that elicit robust B and T cell responses is crucial for vaccine development, especially HTL epitopes that enhance the production of cytokines such as IFN-γ, IL-4, and IL-10 since these cytokines facilitate epitope presentation to HTLs via MHC class II molecules [37]. Importantly, most immune cells, except memory cells, undergo apoptosis following infection resolution. The primary objective of this study was to identify protein epitopes capable of activating both humoral and cellular immunity, predicted from experimental data using the Immune Epitope database (IEDB) [40]. Linear B-cell epitopes were predicted using ABCpred, a synthetic intelligence-based automated learning tool. To ensure their safety and efficacy, these epitopes were evaluated for antigenicity, hypo-allergenicity, and non-toxicity using appropriate online resources. The current vaccine design incorporated epitopes associated with various MHC alleles, and molecular docking was performed on six selected epitopes to assess binding affinity and facilitate robust ligand-receptor interactions. This molecular docking approach allowed us to quantify interaction energies, with lower energy levels indicating stronger binding between ligand and receptor. This study demonstrated the vaccine's potential to elicit an immune response, showing high affinity for TLR-2, TLR-4, TLR-5, and TLR-9. Additionally, extensive molecular dynamics simulations (iMOD) were conducted to evaluate the overall stability of the complex, and immune-informatics methods were used to evaluate the stability, antigenicity, thermal stability, and hydrophilicity of the mRNA vaccine peptide sequence. The optimized sequence was analyzed for cryptic splice sites using ESEfinder (none detected) and secondary structures using RNAfold; the 5' UTR showed no stable hairpins near the cap (minimum free energy of -449.70 kcal/moL for the full construct). The Kozak sequence (GCCACC) and a long Poly(A) tail (120 nt) were included to enhance translation and stability.

Overall, this study offers several distinct advances over previous *H. pylori* multi-epitope vaccine designs. First, unlike prior subunit vaccines, an mRNA-based construct was designed, incorporating a 5′/3′ UTR, a Kozak sequence, and an MITD domain for enhanced translation and MHC-I presentation. Second, proteome-wide screening was performed rather than pre-selecting a handful of antigens. Third, the adjuvant (RpfE) and linker combination (EAAAK/GPGPG/KK/AAY) has not been previously applied to *H. pylori* vaccine designs. Finally, TLR2/4/5/9 docking and full molecular dynamics were included, providing broader immune activation predictions than earlier reports.

The findings indicated that the immunological vaccine, administered in three doses, resulted in increased B and T cell counts and elevated IFN-γ production, signifying robust cellular immunity. Furthermore, the observed dendritic and macrophage activity

suggests the establishment of immunological memory. Therefore, the developed vaccine could be a promising option for treating *H. pylori* infections.

Conclusion

H. pylori is a major contributor to gastrointestinal disorders, prompting the computational design of a novel multi-epitope mRNA vaccine using immune-informatics to potentially elicit both humoral and cellular immunity. Various in silico techniques, including molecular docking and thermodynamic stability profiling, predicted the desired vaccine stability and immune response features. Based on the findings, the vaccine is computationally predicted to exhibit favorable physicochemical properties and induce an immune response. However, these computational predictions require validation through in vitro and in vivo studies before any clinical potential could be claimed.

Acknowledgements

Not applicable.

Authors' contributions: The study was designed by B.S. K. and N.S.; the methodology was carried out by M.H.M. and S.Kh. The manuscript was drafted by M.Y. and revised by N.O. All authors read and approved the manuscript.

Ethical approval: This study was approved by the Ethical Committee of Ilam University of Medical Sciences and supported by Student Research Committee (Ethical code: IR.MEDILAM.REC.1403.166).

Consent for publication: All authors declare their consent to publish the manuscript.

Funding: Not applicable.

Availability of data and materials: All the datasets supporting the conclusions of this article are available. Additional data from this paper could be obtained upon request. The corresponding author (Behrooz Sadeghi Kalani.: Behroz.sadeghi@gmail.com) should be contacted if someone wishes to ask for this study data.

Competing interests: The authors declare that they have no conflict of interest.

Declaration of Artificial Intelligence (AI) Use: ChatGPT-4o was used solely to edit a limited number of sentences of the article's text to improve its fluency.

Abbreviations

CDI: *H. pylori* infection
RNA: Ribonucleic acid
CTL: Cytotoxic T lymphocytes
HTL: Helper T lymphocyte
mRNA: Messenger RNA
BLAST: Basic local alignment search tool
MHC: Major histocompatibility complex
ORF: Open reading frame
PSIPRED: Position specific iterated prediction
ElliPro*:* Antibody Epitope Prediction
CDS: Coding sequence
CAI: Codon Adaptation Index
MFE: Minimum free energy
TLRs: Toll-like receptors
MD: Molecular dynamics
RMSD: Root mean square deviation
PSSM: Position specific scoring matrix
IEDB: Immune epitope database

References

1. Yi, M., et al., Helicobacter pylori infection process: from the molecular world to clinical treatment. Frontiers in Microbiology, 2025. 16: p. 1541140.
2. Duan, Y., et al., Helicobacter pylori and gastric cancer: mechanisms and new perspectives. Journal of Hematology & Oncology, 2025. 18(1): p. 10.
3. Ali, A. and K.I. AlHussaini, Helicobacter pylori: a contemporary perspective on pathogenesis, diagnosis and treatment strategies. Microorganisms, 2024. 12(1): p. 222.
4. Elbehiry, A., et al., Helicobacter pylori infection: current status and future prospects on diagnostic, therapeutic and control challenges. Antibiotics, 2023. 12(2): p. 191.

5. Ibrahim, M.E., Epidemiology, pathogenicity, risk factors, and management of Helicobacter pylori infection in Saudi Arabia. Biomolecules and Biomedicine, 2024. 24(3): p. 440.
6. Mladenova, I., Review–Epidemiology of Helicobacter pylori infection. Microb Health Dis, 2023. 5: p. e913.
7. Wizenty, J. and M. Sigal, Helicobacter pylori, microbiota and gastric cancer—Principles of microorganism-driven carcinogenesis. Nature Reviews Gastroenterology & Hepatology, 2025. 22(5): p. 296-313.
8. Sun, Q., et al., Helicobacter pylori infection: a dynamic process from diagnosis to treatment. Frontiers in cellular and infection microbiology, 2023. 13: p. 1257817.
9. Chey, W.D., et al., ACG clinical guideline: treatment of Helicobacter pylori infection. Official journal of the American College of Gastroenterology| ACG, 2024. 119(9): p. 1730-1753.
10. Kadhim, A.S. and A.S. Al-Karawi, Insights into the pathogenesis, virulence factors, and diagnosis of Helicobacter pylori: A comprehensive review. American Journal of Bioscience and Bioinformatics, 2023. 2(1): p. 31-37.
11. Sharndama, H.C. and I.E. Mba, Helicobacter pylori: an up-to-date overview on the virulence and pathogenesis mechanisms. Brazilian Journal of Microbiology, 2022. 53(1): p. 33-50.
12. Wang, H., et al., A review of signal pathway induced by virulent protein CagA of Helicobacter pylori. Frontiers in cellular and infection microbiology, 2023. 13: p. 1062803.
13. Liu, S., et al., Helicobacter pylori CagA promotes gastric cancer immune escape by upregulating SQLE. Cell Death & Disease, 2025. 16(1): p. 17.
14. Karbalaei, M., A. Talebi Bezmin Abadi, and M. Keikha, Clinical relevance of the CagA and VacA s1m1 status and antibiotic resistance in Helicobacter pylori: a systematic review and meta-analysis. BMC Infectious Diseases, 2022. 22(1): p. 573.
15. Son, Y.S., et al., Helicobacter pylori VacA-induced mitochondrial damage in the gastric pit cells of the antrum and therapeutic rescue. Biomaterials, 2025. 314: p. 122842.
16. Yunle, K., et al., Advances in Helicobacter pylori vaccine research: From candidate antigens to adjuvants—A review. Helicobacter, 2024. 29(1): p. e13034.
17. Keshri, A.K., et al., Designing and development of multi-epitope chimeric vaccine against Helicobacter pylori by exploring its entire immunogenic epitopes: an immunoinformatic approach. BMC bioinformatics, 2023. 24(1): p. 358.
18. Gong, J., et al., Helicobacter pylori vaccine: Mechanism of pathogenesis, immune evasion and analysis of vaccine types. Vaccines, 2025. 13(5): p. 526.
19. Raman, S.K.S., et al., In silico design of a VacA-Based Multi-Epitope subunit vaccine candidate for immunoprotection against Helicobacter pylori. Human Immunology, 2026. 87(6): p. 111741.
20. Asadinezhad, M., et al., Development of innovative multi-epitope mRNA vaccine against Pseudomonas aeruginosa using in silico approaches. Briefings in Bioinformatics, 2024. 25(1): p. bbad502.
21. Asadollahi, P. and B.S. Kalani, Novel toxin-based mRNA vaccine against Clostridium perfringens using in silico approaches. Toxicon, 2024. 238: p. 107584.
22. Asadinezhad, M., et al., Proteomics exploration of Brucella melitensis to design an innovative multi-epitope mRNA vaccine. Bioinformatics and Biology Insights, 2024. 18: p. 11779322241272404.
23. Fattahi, R., et al., Computational Design of Inhibitory Peptides and an mRNA-Based Multi-Epitope Vaccine Targeting the MIC3 Protein of Eimeria tenella. Experimental Parasitology, 2025: p. 108986.
24. Fattahi, N., et al., Engineering a novel multi-epitope mRNA vaccine against major bacterial meningitis pathogens: E. coli K1, group B Streptococcus, Listeria monocytogenes, neisseria meningitidis, and Streptococcus pneumoniae. International Journal of Biological Macromolecules, 2025. 317: p. 144311.
25. Al-Sallami, D., et al., Design of Innovative Divalent Cj1621 and CjaA Multiepitope mRNA-Based Vaccine Against Foodborne Campylobacter jejuni Using In Silico Approaches. Veterinary Medicine International, 2025. 2025(1): p. 3487209.
26. Fattahi, R. and B. Sadeghi Kalani, mRNA vaccine design using the proteome of Theileria annulata through immunoinformatics approaches. Msphere, 2025. 10(5): p. e00809-24.
27. Cruz, J., et al., BacMap: an up-to-date electronic atlas of annotated bacterial genomes. Nucleic acids research, 2012. 40(D1): p. D599-D604.
28. Sabzi, S., et al., Genome-wide subtraction analysis and reverse vaccinology to detect novel drug targets and potential vaccine candidates against ehrlichia chaffeensis. Applied Biochemistry and Biotechnology, 2023. 195(1): p. 107-124.
29. Praveen, M., Multi-epitope-based vaccine designing against Junín virus glycoprotein: immunoinformatics approach. Future Journal of Pharmaceutical Sciences, 2024. 10(1): p. 29.
30. Cui, M., et al., Design of a Helicobacter pylori multi-epitope vaccine based on immunoinformatics. Frontiers in Immunology, 2024. 15: p. 1432968.

Frontiers in Immunology, 2024. 15: p. 1432968.
31. Alhassan, H.H., Advanced vaccinomic, immunoinformatic, and molecular modeling strategies for designing Multi-epitope vaccines against the Enterobacter cloacae complex. Frontiers in Immunology, 2024. 15: p. 1454394.
32. López-Blanco, J.R., et al., iMODS: internal coordinates normal mode analysis server. Nucleic acids research, 2014. 42(W1): p. W271-W276.
33. Ghosh, P., et al., A novel multi-epitopic peptide vaccine candidate against Helicobacter pylori: in-silico identification, design, cloning and validation through molecular dynamics. International journal of peptide research and therapeutics, 2021. 27: p. 1149-1166.
34. Khan, M., et al., Immunoinformatics approaches to explore Helicobacter Pylori proteome (Virulence Factors) to design B and T cell multi-epitope subunit vaccine. Scientific reports, 2019. 9(1): p. 13321.
35. Barbier, A.J., et al., The clinical progress of mRNA vaccines and immunotherapies. Nature biotechnology, 2022. 40(6): p. 840-854.
36. Pardi, N., et al., mRNA vaccines—a new era in vaccinology. Nature reviews Drug discovery, 2018. 17(4): p. 261-279.
37. Shahrear, S. and A.B.M.M.K. Islam, Modeling of MT. P495, an mRNA-based vaccine against the phosphate-binding protein PstS1 of Mycobacterium tuberculosis. Molecular Diversity, 2023. 27(4): p. 1613-1632.